Disturbance-free distributed Bragg reflector laser-diode interferometer with a double sinusoidal phase-modulating technique for measurement of absolute distance

Takamasa Suzuki, Takao Ohizumi, Tatsuhiko Sekimoto, and Osami Sasaki

A new range-finding technique that uses both double sinusoidal phase modulation and quasi-two-wavelength interferometry is described. Two independent interference signals are generated with respect to two different wavelengths on a time-sharing basis. We clarify that external disturbances of these interference signals are eliminated by both feedback control and differential detection and that the feedback control does not affect the distance measurement. A single distributed Bragg reflector laser diode allows us to simplify the optical setup and to improve the measurement accuracy. After discussing a measurement range, we estimate a measurement error by making several measurements. © 2004 Optical Society of America

OCIS codes: 120.3180, 150.5670, 120.3940, 120.5060, 140.2020.

1. Introduction

When we measure a distance that is larger than a half wavelength, we usually need to use two-wavelength interferometry.[1,2] To satisfy this requirement a laser diode (LD) is useful because of its variety of wavelengths.[3,4] A LD also has wavelength tunability, and this property enables us to use different wavelengths with a single LD. For instance, quasi-two-wavelength interferometry (QTWI) that uses a single LD has been proposed, and a step-profile measurement was demonstrated.[5] We have proposed another type of QTWI that uses the phase-locking technique and have demonstrated range finding.[6,7] In these interferometers, two different wavelengths that provide two different phases are generated by feedback control. The phases of the interference signals are alternately controlled to a specific value. In this process external disturbance is eliminated to some degree. Feedback control, however, was used not to eliminate disturbance but mainly for phase locking. Therefore external disturbance affected measurement accuracy. Moreover, in this kind of range finder, improvement of measurement accuracy is difficult because the difference in wavelengths used is small.

Double sinusoidal phase-modulating (DSPM) interferometers[8,9] have also been proposed for distance measurement. In those interferometers, two different sinusoidal signals are used to modulate the interference signal. Distance is measured from the modulation amplitude in the sinusoidal phase-modulating (SPM) interference signal by use of frequency analysis.[10] As the feedback control is used mainly to eliminate disturbance, measurement accuracy is not affected much by mechanical disturbance. The DSPM interferometer, however, requires a wide range of wavelength scanning in the light source to improve measurement accuracy because the modulation amplitude is less sensitive to changes in optical path difference (OPD). In this case a distributed Bragg reflector (DBR) LD[9,11] is useful.

In this paper we propose a disturbance-free range-finding technique based on both the DSPM technique and QTWI that uses a DBR LD. Two SPM interference signals that have different phases are simultaneously generated by the DSPM technique. The distance from two SPM interference signals is measured by QTWI. External disturbance is eliminated by both feedback control and differential detection in

The authors are with the Faculty of Engineering, Niigata University, 8050 Ikarashi 2, Niigata, 950-2181 Japan. T. Suzuki's e-mail address is takamasa@eng.niigata-u.ac.jp.

Received 2 March 2004; revised manuscript received 12 May 2004; accepted 21 May 2004.

0003-6935/04/234482-06$15.00/0

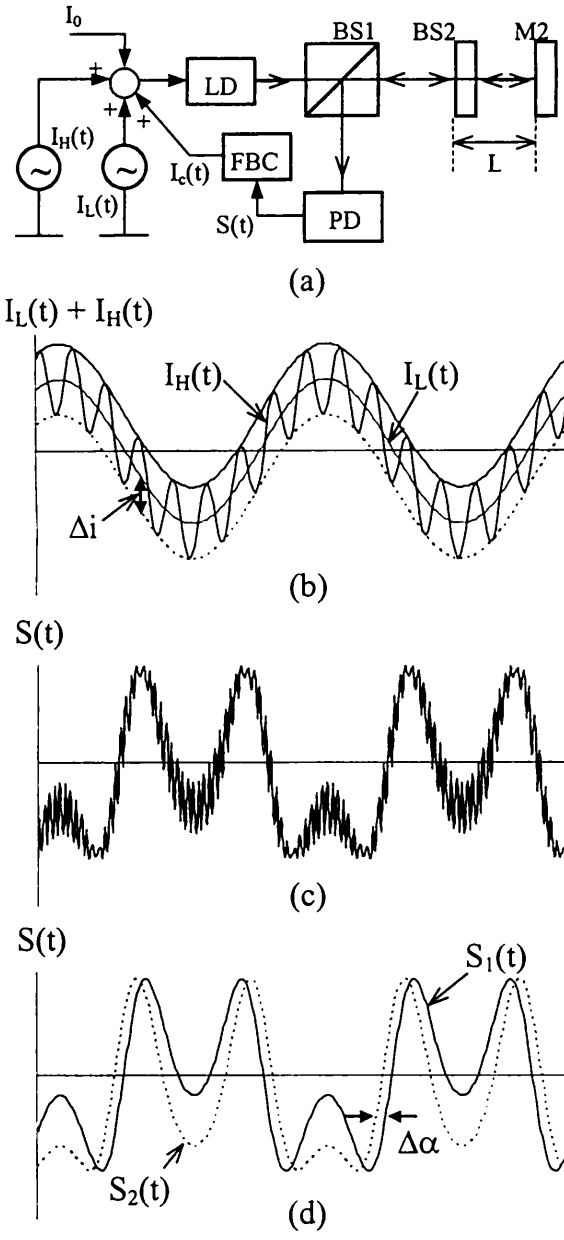

Fig. 1. Schematic of the DSPM technique and QTWI. (a) Basic architecture of the system: BS1, BS2, beam splitters; M2, mirror; FBC, feedback controller; PD, photodetector. (b) Modulating current for the DSPM technique, (c) DSPM interference signal, (d) separated interference signals for the QTWI.

QTWI. We explain that differential detection also enables us to implement distance measurement under feedback control. The results of several experiments indicate that the measurement error is 0.85 μm at an OPD of ~2.6 mm.

2. Measurement System

A. DSPM Interference Signal

A schematic of the system that we propose is shown in Fig. 1. The OPD of the Fizeau interferometer illustrated in Fig. 1(a) is $2L$. The injection current for the LD consists of dc bias current I_0, which determines central wavelength λ_0, a low-frequency modulation current

$$I_L(t) = m \cos(\omega_c t + \theta), \tag{1}$$

a high-frequency modulation current

$$I_H(t) = \Delta i \cos(n\omega_c t), \tag{2}$$

and control current $I_c(t)$. The frequency of $I_H(t)$ is n times as large as that of $I_L(t)$, where n is an integer. When the sum of $I_L(t)$ and $I_H(t)$ that is schematically shown in Fig. 1(b) is injected into the LD, we have a so-called DSPM interference signal[8,9]:

$$S(t) = a + b \cos[Z_L \cos(\omega_c t + \theta) + Z_H \cos(n\omega_c t) + \alpha_0 + \delta(t)], \tag{3}$$

where a and b are the dc components and the amplitudes of the ac component, respectively,

$$Z_L = 4\pi L\beta m/\lambda_0^2, \tag{4}$$

$$Z_H = 4\pi L\beta\Delta i/\lambda_0^2 \tag{5}$$

are the modulation amplitudes that correspond to $I_L(t)$ and $I_H(t)$, respectively, and

$$\alpha_0 = 4\pi L/\lambda_0 \tag{6}$$

and $\delta(t)$ are the initial phase that depends on OPD $2L$ and the phase deviation caused by the external disturbance, respectively. β represents the ratio between the wavelength change and the injection current; it is referred to as modulation efficiency.

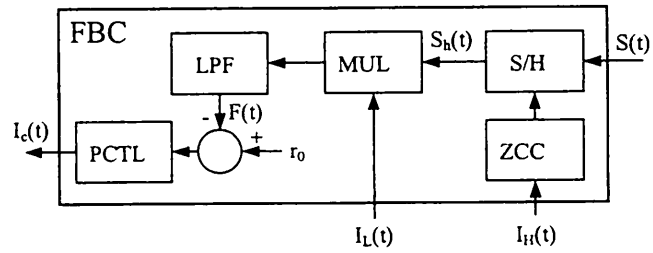

Fig. 2. Block diagram of the feedback controller: S/H, sample-and-hold circuit; ZCC, zero-cross circuit; MUL, multiplier; LPF, low-pass filter; PCTL, proportional controller; FBC, feedback controller.

B. Feedback Control

Assuming that the major source of error in distance measurement in our system is the OPD's temporal change $d(t)$, $\delta(t)$ is expressed by

$$\delta(t) = 4\pi d(t)/\lambda_0. \tag{7}$$

Even if $d(t)$ is smaller than $\lambda_0/2$, it affects the phase of the interference signal. It results in an error in phase measurement. Therefore we equipped our system with a feedback controller to eliminate disturbance, as shown in Fig. 1(a). Figure 2 is a block diagram of the feedback controller. When $S(t)$ is

sampled and held at the time when $I_H(t) = 0$, we simply obtain a single SPM interference signal:

$$S_h(t) = a + b \cos[Z_L \cos(\omega_c t + \theta) + \alpha_0 + \delta(t)]. \quad (8)$$

$S_h(t)$ is equivalent to the interference signal that is modulated only by $I_L(t)$. The sample-and-hold pulse is produced from $I_H(t)$ by use of a zero-cross circuit. Multiplying $S_h(t)$ by $I_L(t)$ by a multiplier and passing the product through a low-pass filter, we obtain the feedback signal[12]

$$F(t) = K_f \sin[\alpha_0 + \delta(t)], \quad (9)$$

where K_f is a constant.

When we use a proportional controller for feedback control, α_0 and $\delta(t)$ become

$$\alpha_c = \alpha_0 - (4\pi L/\lambda_0^2)\lambda_a, \quad (10)$$

$$\delta_c(t) = \delta(t) - (4\pi L/\lambda_0^2)\lambda_b(t), \quad (11)$$

respectively, where λ_a and $\lambda_b(t)$ are the compensating wavelengths that are generated by the feedback control. They approach zero if we set reference r_0 to zero. Thus feedback control eliminates not only the disturbance but also the OPD information from initial phase α_0. This means that the distance cannot be detected from α_0 when the feedback control is working.

Also, the feedback control changes modulation amplitude Z_H to

$$Z_c = Z_H - (8\pi L\Delta\lambda/\lambda_0^3)[\lambda_a + \lambda_b(t)]. \quad (12)$$

Because the second term in Eq. (12) approaches zero, Z_H is not affected by the feedback control. Therefore we use Z_H for range finding.

C. QTWI with a DSPM Technique

We sample $S(t)$, which is formulated in Eq. (3), at peaks and valleys of $I_H(t)$ under feedback control. The maxima and the minima of $I_H(t)$ equivalently give the offset $\pm\Delta i$ to $I_L(t)$, as shown in Fig. 1(b). This offset current enables us to use two different wavelengths, whose difference is

$$\Delta\lambda = 2\beta\Delta i. \quad (13)$$

This technique is QTWI. Thus, as shown in Fig. 1(c), we simultaneously obtain two independent interference signals:

$$S_i(t) = a + b \cos[Z_L \cos(\omega_c t + \theta) + \alpha_i] \quad (i = 1, 2), \quad (14)$$

where

$$\alpha_1 = \alpha_c + Z_H + \delta_c(t), \quad (15)$$

$$\alpha_2 = \alpha_c - Z_H + \delta_c(t). \quad (16)$$

$S_1(t)$ and $S_2(t)$ are the discrete data sampled at peaks and valleys, respectively, of $I_H(t)$. If phases α_1 and α_2 are detected with SPM interferometry,[10] difference $\Delta\alpha$ between α_1 and α_2 is represented by

$$\Delta\alpha = 2Z_H, \quad (17)$$

which indicates that the differential detection eliminates not only the offset phase α_c but also the remaining external disturbance $\delta_c(t)$. From Eqs. (5), (13), and (17), the OPD is simply given by

$$L = (\Lambda/4\pi)\Delta\alpha, \quad (18)$$

where

$$\Lambda = \lambda_0^2/\Delta\lambda \quad (19)$$

is a synthetic wavelength that depends on the wavelength scanning range.

D. Error Analysis and Measurement Range

In this section we discuss the measurement error and the range of our system. Differentiating Eq. (18), we have

$$\delta L = (\Lambda/4\pi)\delta(\Delta\alpha), \quad (20)$$

which shows that error in measured distance depends on the accuracy of $\Delta\alpha$.

If we assume that the phases detected by the SPM interferometry are $\alpha_1 \pm \delta\alpha_1$ and $\alpha_2 \pm \delta\alpha_2$, the maximum value of $\delta(\Delta\alpha)$ is given by $\delta(\Delta\alpha)_{max} = \delta\alpha_1 + \delta\alpha_2$ because $\Delta\alpha$ is the phase difference between the phases detected, where $\delta\alpha_1$ and $\delta\alpha_2$ are the deviations from the exact values. The maximum of the measurement error is then given by

$$\delta L_{max} = (\Lambda/4\pi)\delta(\Delta\alpha)_{max}. \quad (21)$$

The maximum of measurement range L_{max} is obviously half of Λ, which we can adjust by varying Δi as shown in Eqs. (13) and (19). The minimum is determined by modulation amplitude Z_L as mentioned in Ref. 9 because the signal processing is based on SPM interferometry.[10]

The minimum measurement range L_{min} is then given by

$$L_{min} = (\lambda_0^2/4\pi\beta m) Z_{Lmin} \quad (22)$$

from Eq. (4), where Z_{Lmin} is the minimum of Z_L.

In Section 3 we provide some estimations of the error and measurement range.

3. Experiment

A. Experimental Setup

Figure 3 shows the experimental setup. A laser beam that radiates from the DBR LD (Yokogawa Model YL85XTW) is fed into a Fizeau interferometer, in which half of OPD L is ~2.6 mm. Central wavelength λ_0 and the maximum output power of the DBR LD are 853.5 nm and 10 mW, respectively. Modulation efficiency β was measured as 5.07×10^{-3} nm/mA. The DBR LD consists of an active layer, a phase-tuning layer, and a reflection-tuning layer.[9] Each layer has an electrode that injects forward cur-

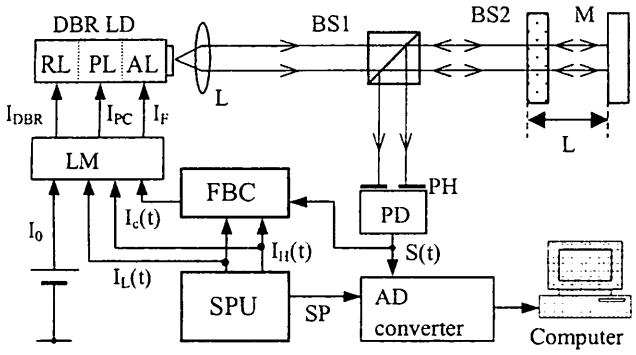

Fig. 3. Experimental setup: L's, lenses; BS1, BS2, beam splitters; M, mirror; FBC, feedback controller; PH, pinhole; PD, photodetector; SPU, signal-processing unit; LM, laser-diode modulator; RL, reflection-tuning layer; PL, phase-tuning layer; AL, active layer; AD, analog to digital.

rent I_F, phase-tuning current I_{PC}, and the reflection-tuning current I_{DBR}. These currents are supplied by a laser modulator. The laser modulator also maintains the ratio between I_{PC} and I_{DBR} at 1:1.4. The interference signal detected by the photodetector is saved into a computer through an analog-to-digital converter. The signal-processing unit supplies the sampling pulse and modulating currents $I_L(t)$ and $I_H(t)$.

A block diagram of the signal-processing unit is shown in Fig. 4. It has two sinusoidal oscillators that supply $I_H(t)$ and $I_L(t)$, respectively. OSC2 is equipped with an external trigger input that is synchronized with the other oscillator. The frequencies of $I_H(t)$ and $I_L(t)$ are 64 and 1 kHz, respectively. The 1/64 divider generates a 1-kHz rectangular signal from $I_H(t)$ and feeds it into the external trigger input of OSC2 to synchronize the two oscillators. The sampling pulse generator supplies the sampling pulses at the peaks and the valleys of $I_H(t)$.

B. Experimental Results

Several experiments are described in this section. All experiments were implemented with an iron plate placed on a workbench.

We first observed a modulating signal and an interference signal. The results are shown in Fig. 5. Figures 5(a), 5(b), and 5(c) correspond, respectively,

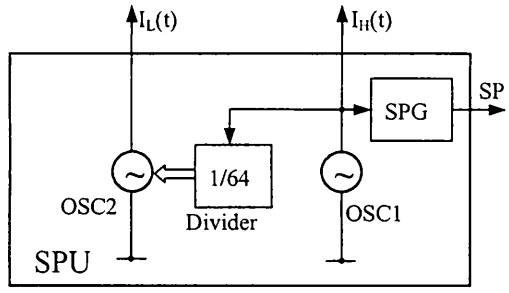

Fig. 4. Block diagram of the signal-processing unit: OSC1, OSC2, oscillators; SPG, sampling pulse generator; SP, sampling pulse; SPU, signal-processing unit.

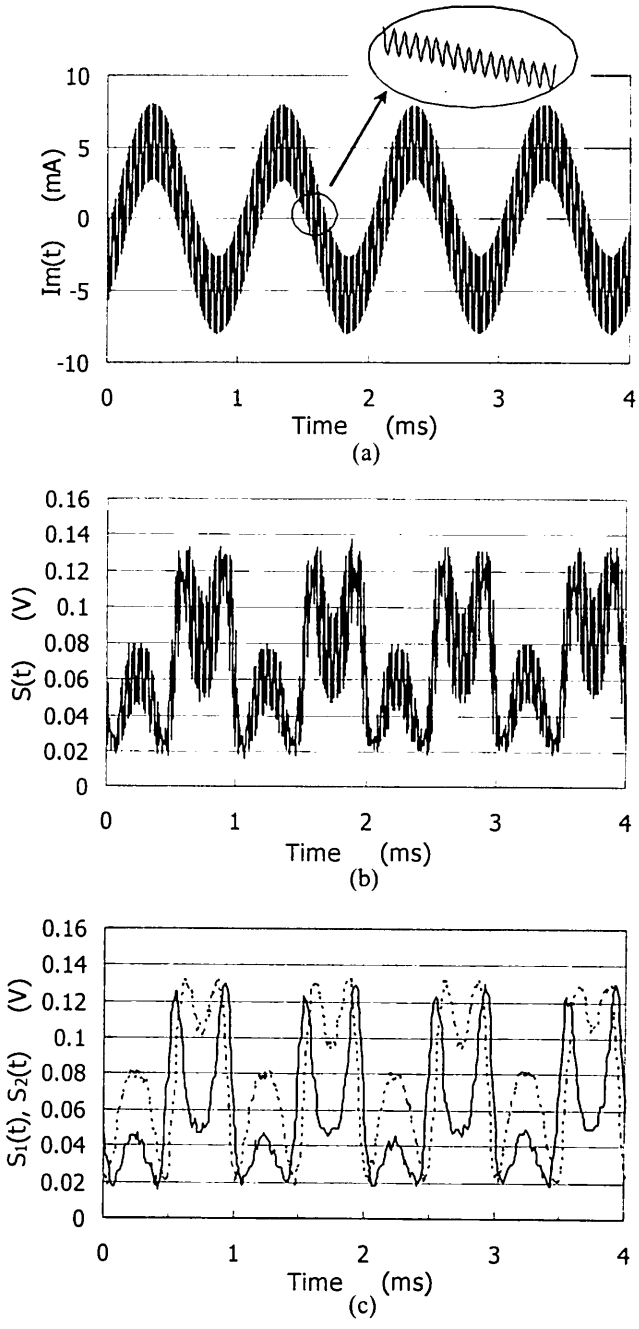

Fig. 5. Observations of (a) a DSPM signal, (b) a DSPM interference signal, and (c) a separate DSPM interference signal for QTWI.

to Figs. 1(b), 1(c), and 1(d). Figure 5(a) shows the observed DSPM signal. Higher-frequency signal $I_H(t)$ is superimposed onto lower-frequency signal $I_L(t)$. Part of Fig. 5(a) is magnified in the inset. The amplitudes of $I_L(t)$ and $I_H(t)$ were 5 and 2.5 mA, respectively. DSPM interference signal $S(t)$ is traced in Fig. 5(b). The waveform is not so clear because two interference signals, $S_1(t)$ and $S_2(t)$, overlap. These signals are clearly shown in Fig. 5(c) by a solid curve and a dashed curve, respectively, when odd and even numbers of data are extracted. The phase difference between $S_1(t)$ and $S_2(t)$ is proportional to distance L.

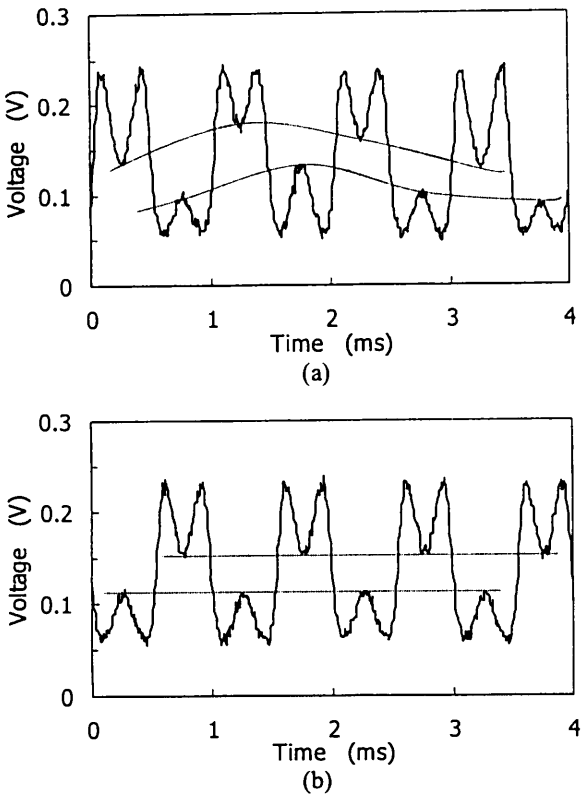

Fig. 6. Interference signals observed when the feedback control is (a) off and (b) on. Dotted curves indicate the phase deviation caused by the external disturbance.

Next we confirmed the elimination of disturbance by feedback control. The observed interference signals are shown in Fig. 6. The interference signal that was significantly affected by external disturbance when the feedback control was off is shown by dotted curves in Fig. 6(a). When the feedback control was on, however, these phase deviations were eliminated, as shown in Fig. 6(b). These observations confirm that the feedback signal generated by the sampling technique functions well and that the disturbance is eliminated.

Finally, we estimated range and measurement error and demonstrated the measurement of absolute distance. In the experiment the amplitudes of $I_L(t)$ and $I_H(t)$ were m = 12 mA and Δi = 11 mA, respectively. Wavelength difference $\Delta\lambda$ and synthetic wavelength Λ calculated from Eqs. (13) and (19) were 1.12×10^{-1} nm and 6.5 mm, respectively.

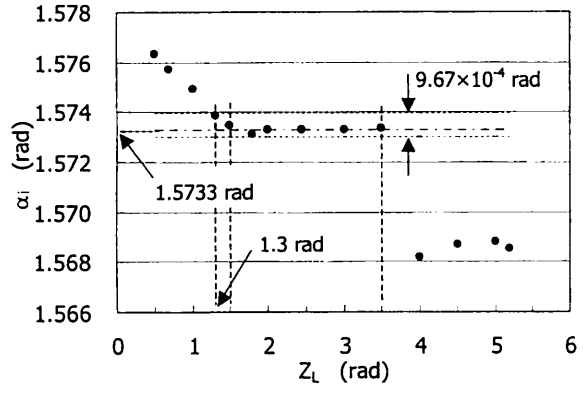

Fig. 7. Numerical calculation of phase detection with respect to Z_L in SPM interferometry.

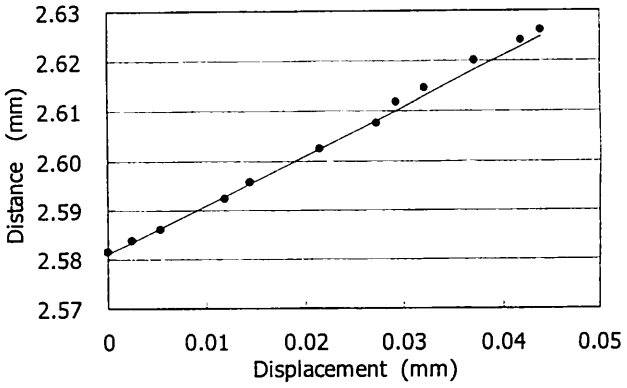

Fig. 8. Absolute distance measured at $L \sim 2.6$ mm.

We used the conditions described above in our estimation. When we set α_i at 1.5733 rad and varied Z_L in Eq. (14), the values of α_i shown in Fig. 7 were detected. If we assume that an allowable maximum error is δL_{max} = 0.5 μm, $\delta(\Delta\alpha)_{max}$ must be less than 9.67×10^{-4} rad from Eq. (21). When Z_L lies in the region from 1.3 to 3.5, this requirement is satisfied, as shown in Fig. 7. Substituting Z_{Lmin} = 1.3 into Eq. (22), we have L_{min} = 1.07 mm, while L_{max} is $\Lambda/2$ = 3.25 mm.

We can find that $\delta(\Delta\alpha)_{max}$ is 7.00×10^{-4} when Z_L is in the region mentioned above. The measurement error is then given by 0.36 μm. If Z_L lies in the region from 1.5 to 3.5, the measurement error is reduced to 0.16 μm because $\delta(\Delta\alpha)_{max}$ becomes 3.00×10^{-4}.

The final experiment measures distance. We moved M along the optical axis with an x-axis stage. The displacement was monitored with a dedicated sensor whose resolution was 0.1 μm. The results are shown in Fig. 8. The solid line is a theoretical line whose inclination is 1. The deviation between the measurements and the solid line is estimated as 0.85 μm rms. The difference between the actual measurement and the theoretical estimation suggests that the external disturbance still remains in the captured interference signal. We believe that appropriate adjustment of the parameters in the feedback control system may reduce the measurement error.

4. Conclusions

We have proposed a disturbance-free range finder based on a double sinusoidal phase-modulating technique and quasi-two-wavelength interferometry. Distance is measured as the phase difference between two SPM interference signals generated by the DSPM technique. The wide range of wavelength tunability of the DBR LD and elimination of distur-

bance by means of both feedback control and differential detection allowed us to measure distance accurately. We clarified that differential detection also enables us to perform distance measurement under feedback control. The measurement error and the range of our system were also discussed and were determined to be 0.16 and 1.07–3.25 mm, respectively, under the conditions of our experiment. In the actual measurement, the error was estimated from several measurements to be 0.85 μm rms.

References

1. J. C. Wyant, "Testing aspherics using two-wavelength holography," Appl. Opt. **10,** 2113–2118 (1971).
2. C. Polhemus, "Two-wavelength interferometry," Appl. Opt. **12,** 2071–2074 (1973).
3. A. J. den Boef, "Two wavelength scanning spot interferometer using single-frequency diode lasers," Appl. Opt. **27,** 306–311 (1988).
4. O. Sasaki, H. Sasazaki, and T. Suzuki, "Two-wavelength sinusoidal phase-modulating laser-diode interferometer insensitive to external disturbances," Appl. Opt. **30,** 4040–4045 (1991).
5. C. C. Williams and K. Wickramasinghe, "Optical ranging by wavelength multiplexed interferometry," J. Appl. Phys. **60,** 1900–1903 (1986).
6. T. Suzuki, O. Sasaki, and T. Maruyama, "Absolute distance measurement using wavelength-multiplexed phase-locked laser diode interferometry," Opt. Eng. **35,** 492–497 (1996).
7. T. Suzuki, T. Muto, O. Sasaki, and T. Maruyama, "Wavelength-multiplexed phase-locked laser diode interferometer using a phase-shifting technique," Appl. Opt. **36,** 6196–6202 (1997).
8. O. Sasaki, T. Yoshida, and T. Suzuki, "Double sinusoidal phase modulating laser diode interferometer for distance measurement," Appl. Opt. **30,** 3617–3621 (1991).
9. T. Suzuki, H. Suda, and O. Sasaki, "Double sinusoidal phase-modulating DBR laser diode interferometer for distance measurement," Appl. Opt. **42,** 60–66 (2003).
10. O. Sasaki and H. Okazaki, "Sinusoidal phase modulating interferometry for surface profile measurement," Appl. Opt. **25,** 3137–3140 (1986).
11. G. Mourat, N. Servagent, and T. Bosch, "Distance measurement using the self-mixing effect in a three electrode distributed Bragg reflector laser diode," Opt. Eng. **39,** 738–743 (2000).
12. O. Sasaki, K. Takahashi, and T. Suzuki, "Sinusoidal phase modulating laser diode interferometer with a feedback control system to eliminate external disturbance," Opt. Eng. **29,** 1511–1515 (1990).